

# EVAPORATING BLACK HOLES IN THE PRESENCE OF DARK SECTORS

Aidan Symons

With  
Michael Baker and Andrea Thamm  
at  
The University of Massachusetts, Amherst

## Talk Outline

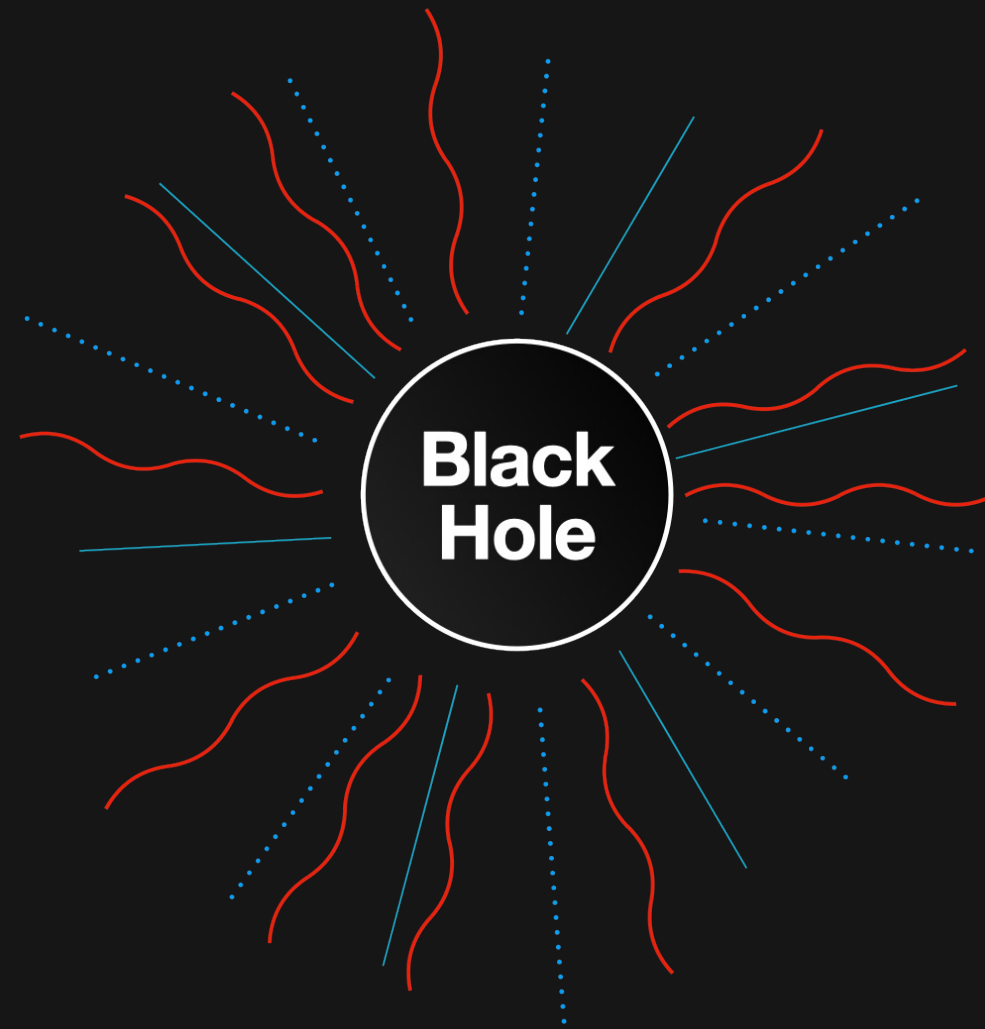
Introduction

Hawking radiation

EBH observational characteristics

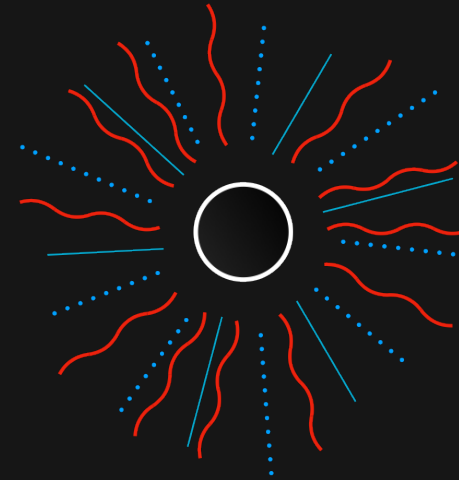
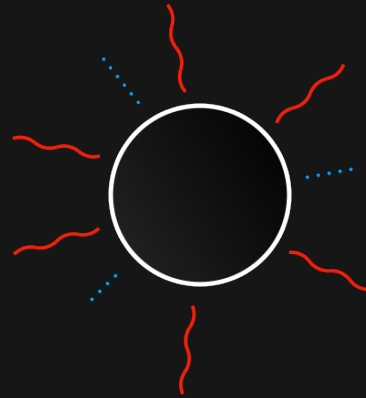
# Introduction

# Introduction



# Introduction

$$T_{BH} \propto \frac{1}{M_{BH}}$$



Time →

## Introduction

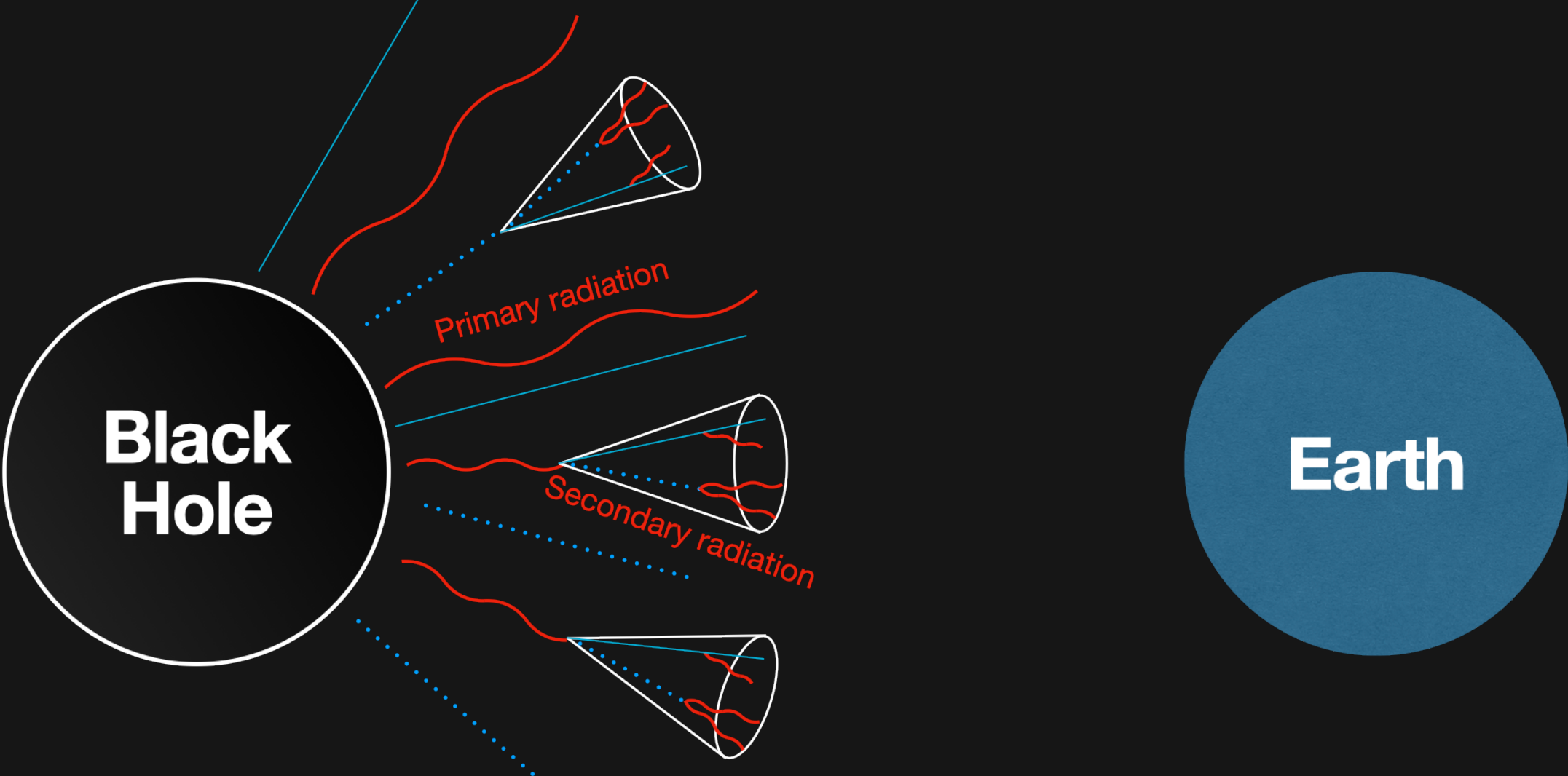
Hawking Radiation = Gravitational

Species  $i$  emitted if  $T_{BH} \gtrsim m_i$

**All** fundamental particles eventually influence spectra

# Hawking radiation

# Hawking Radiation





## Hawking Radiation

Primary radiation

$$\frac{d^2 N_{prim}}{dE dt} = \frac{1}{2\pi\hbar} \frac{\Gamma(E, M_{BH}, s)}{e^{E/kT} \pm 1} n_{dof}$$

Secondary radiation

$$\frac{d^2 N_{sec}}{dE dt} = \sum_i \int_0^\infty dE' \frac{d^2 N_i^{primary}}{dE' dt} \frac{dN_{i \rightarrow s}}{dE}$$

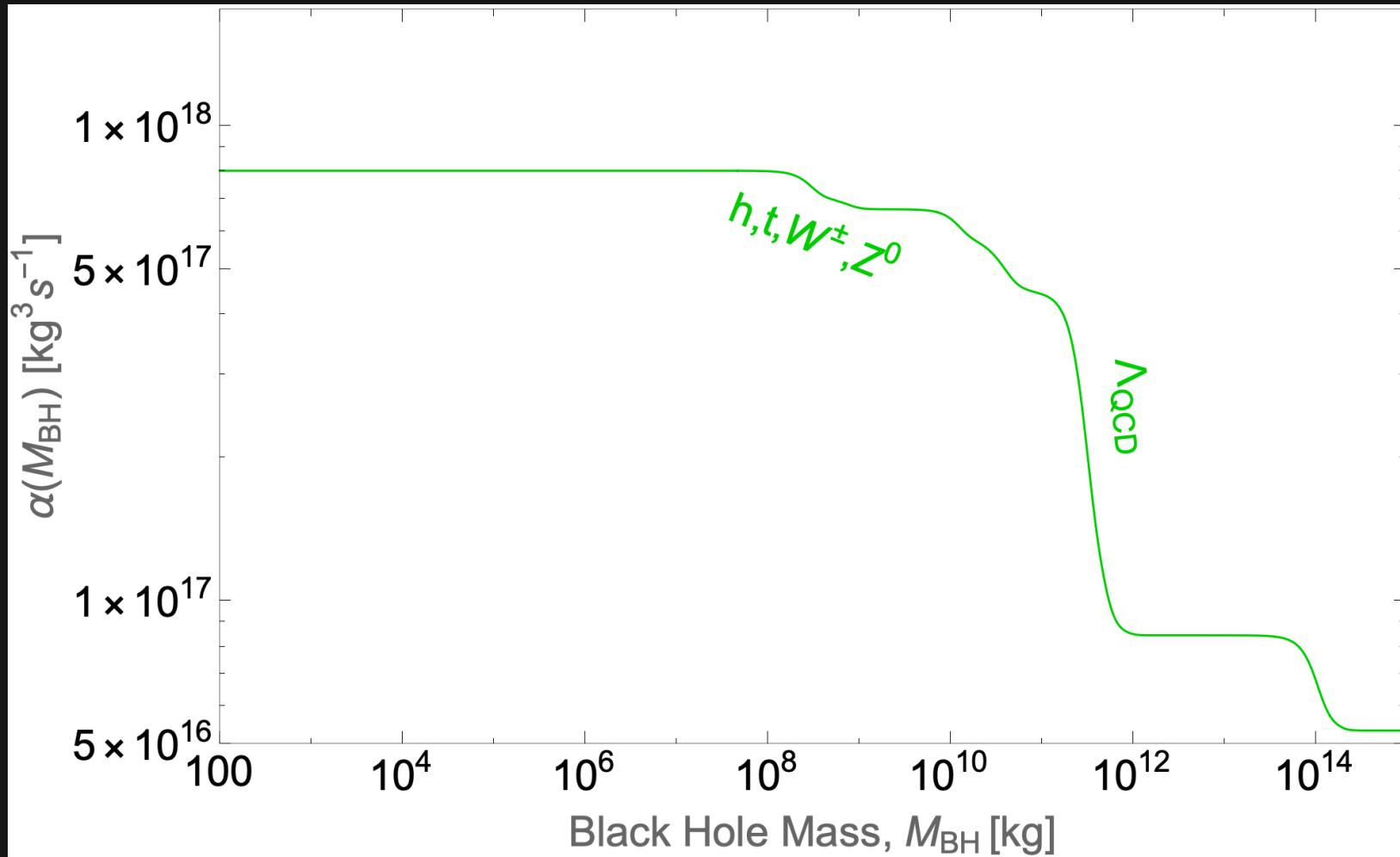
## Hawking Radiation

$$\frac{dM_{BH}}{dt} = - \frac{\alpha(M_{BH})}{M_{BH}^2}$$

$$\alpha(M_{BH}) \propto \sum_i \int_0^\infty \frac{d^2 N_i^{primary}}{dE dt} E dE$$

Sum over **all** particles,  $i$

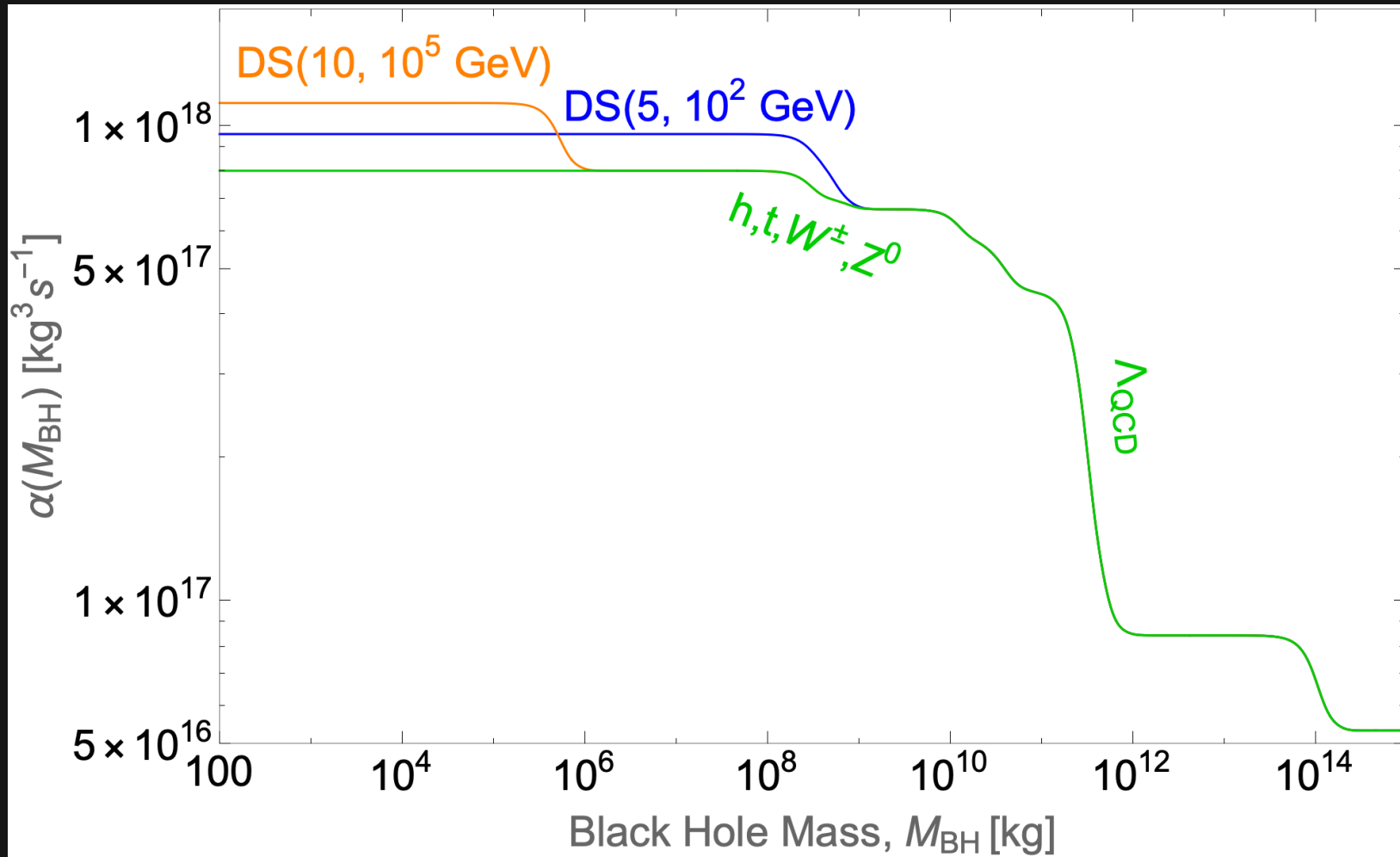
# Hawking Radiation



$$\frac{dM_{BH}}{dt} = -\frac{\alpha(M_{BH})}{M_{BH}^2}$$

$$\alpha(M_{BH}) \propto \sum_i \int_0^\infty \frac{d^2 N_i}{dE dt} E dE$$

# Hawking Radiation



$$\frac{dM_{BH}}{dt} = - \frac{\alpha(M_{BH})}{M_{BH}^2}$$

$$\alpha(M_{BH}) \propto \sum_i \int_0^\infty \frac{d^2 N_i}{dE dt} E dE$$

# Observational characteristics

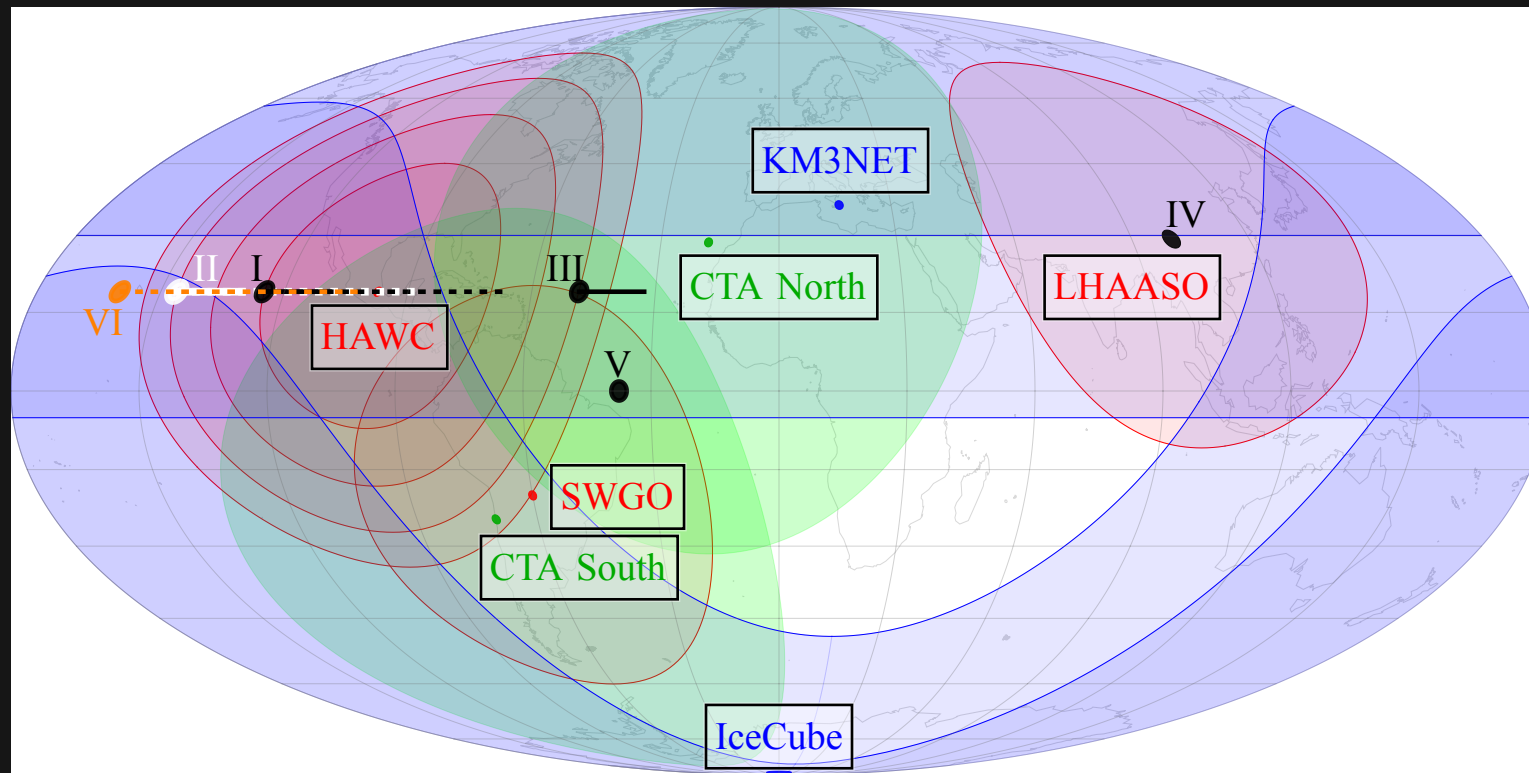
## Observational characteristics

Compute time bins assuming SM and DS

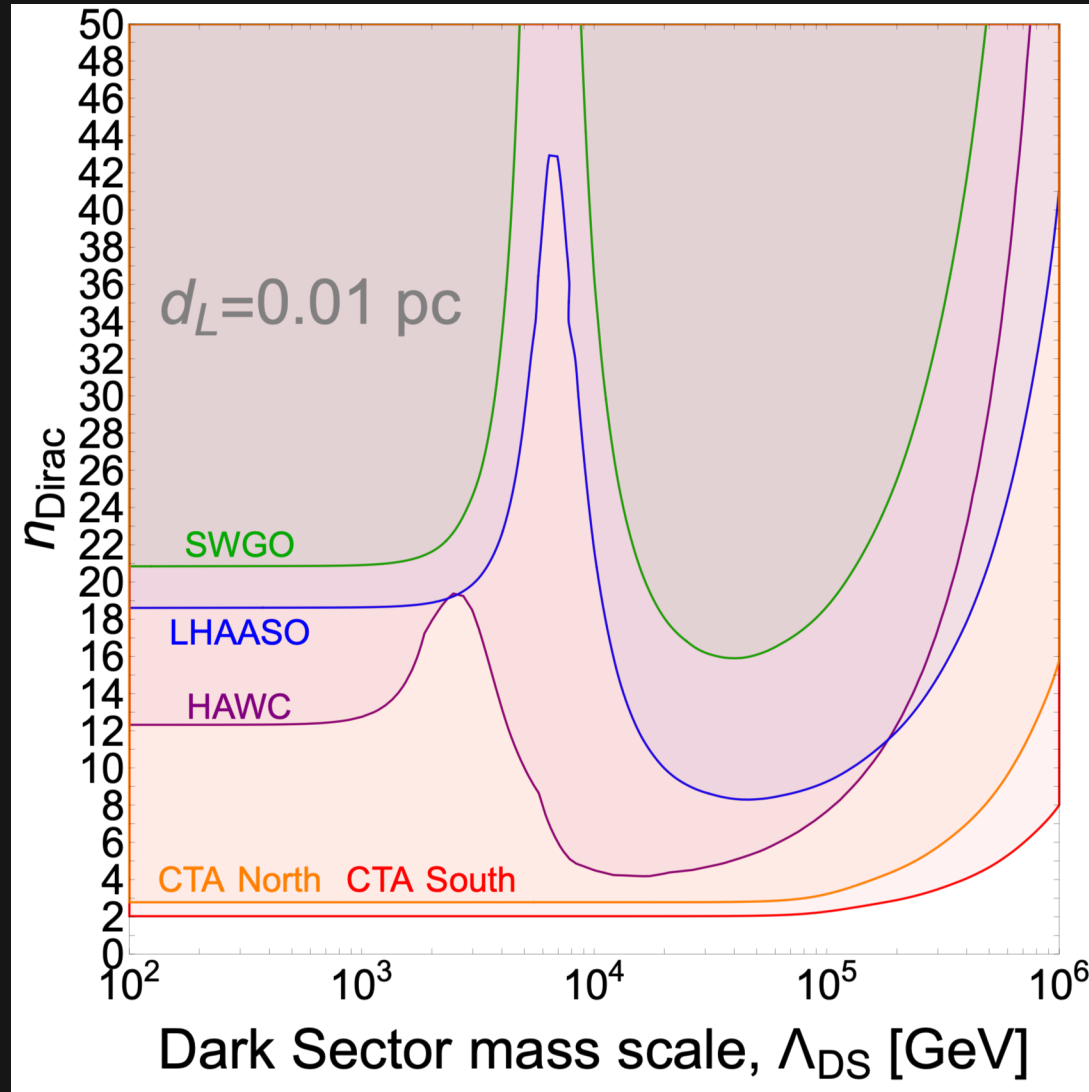
$$N = \frac{1}{4\pi d^2} \int dE A_{eff}(E) \int dt \frac{d^2 N_{total}}{dE dt} (M_{BH}(t), E)$$

Compare SM and DS predictions with a statistical test

# Observational characteristics

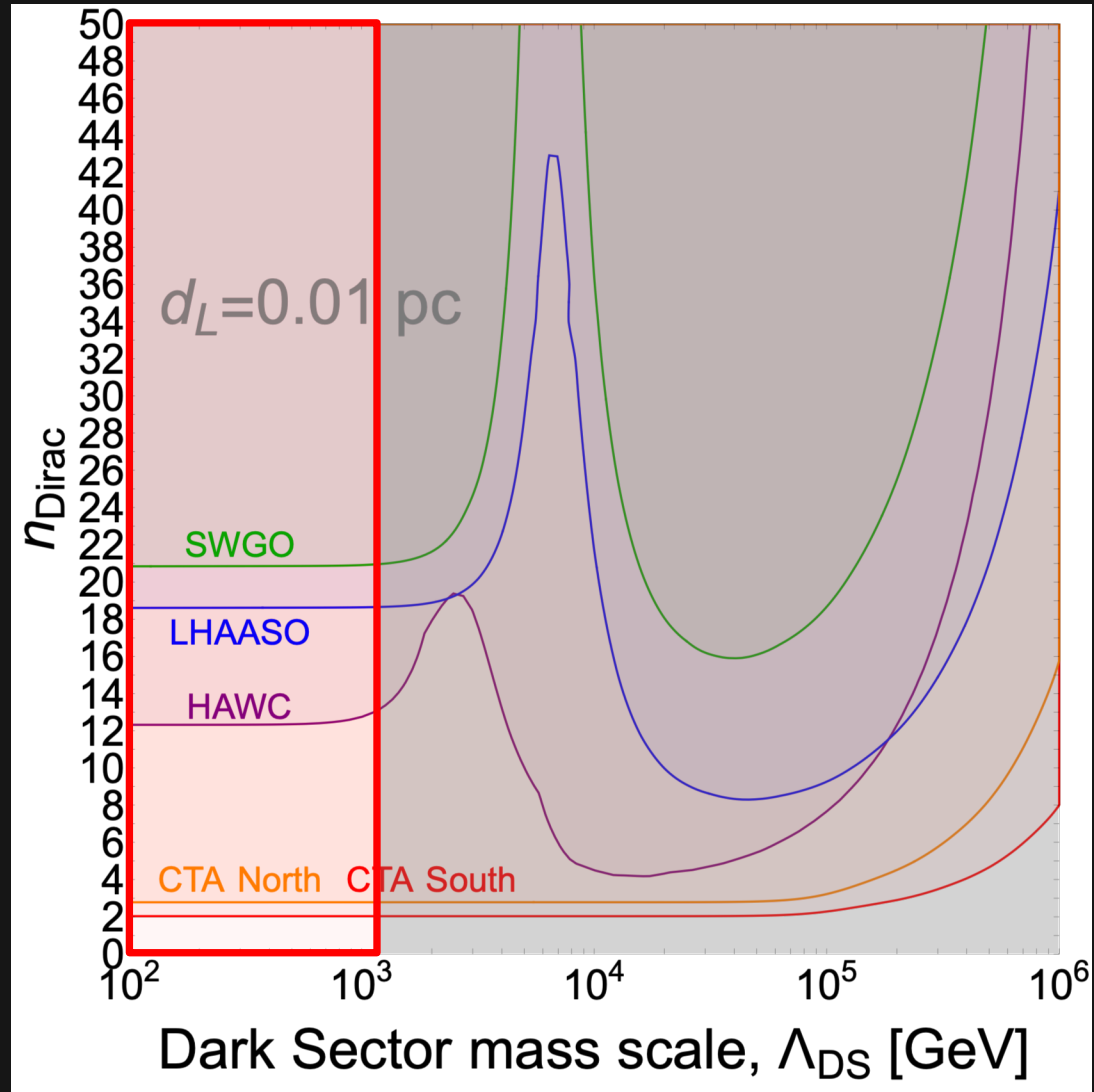


# Observational characteristics

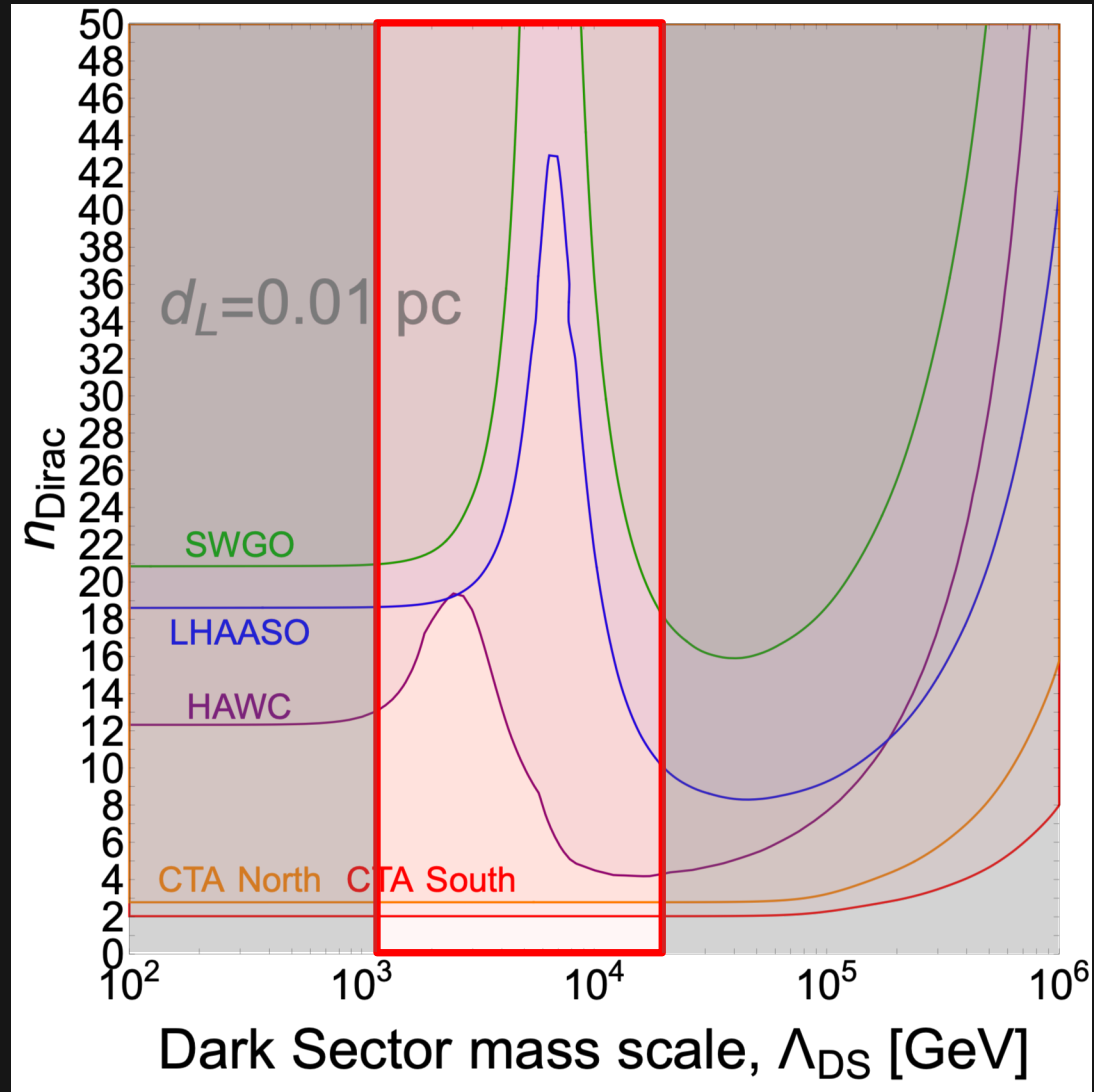




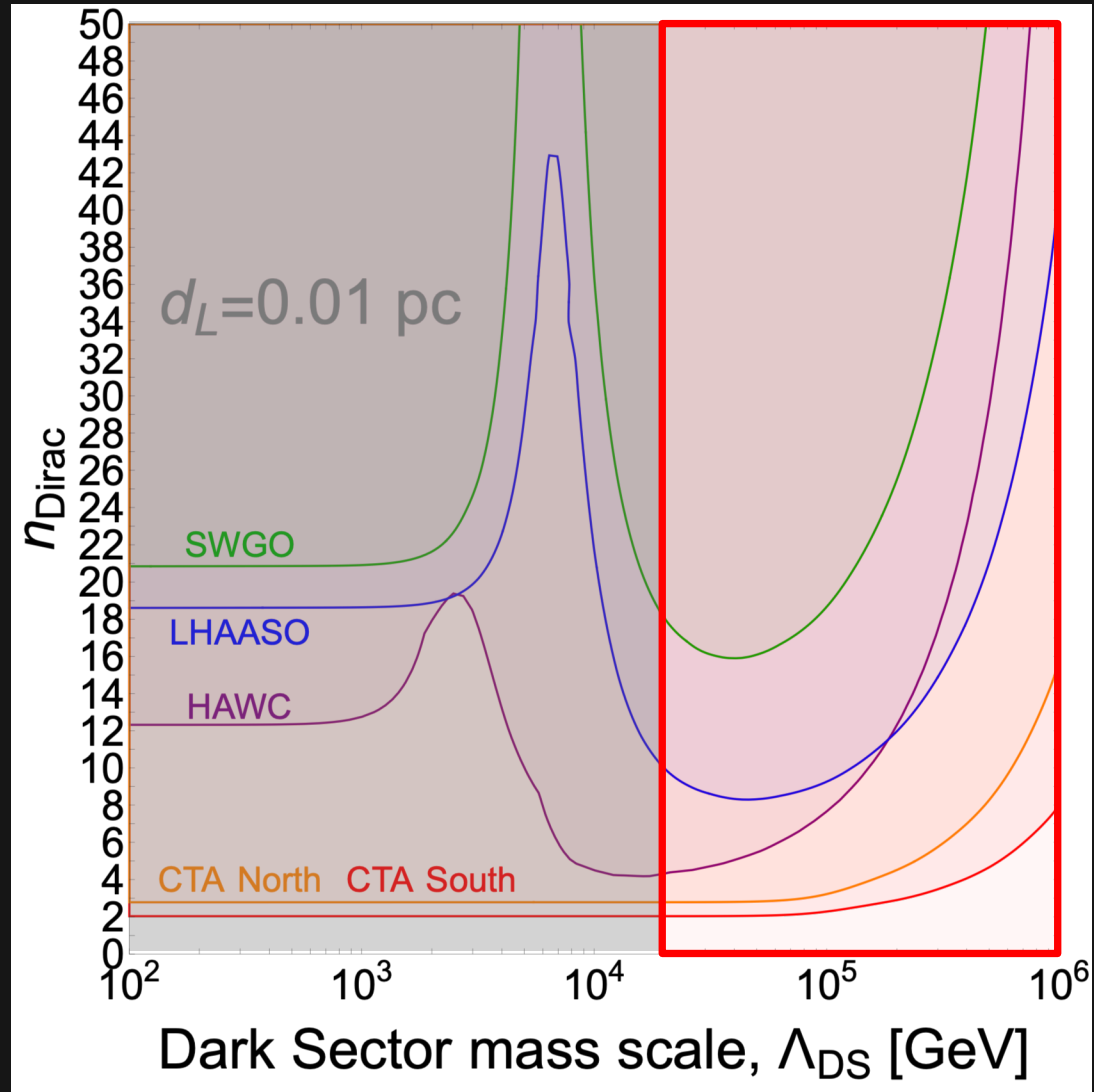
# Observational characteristics



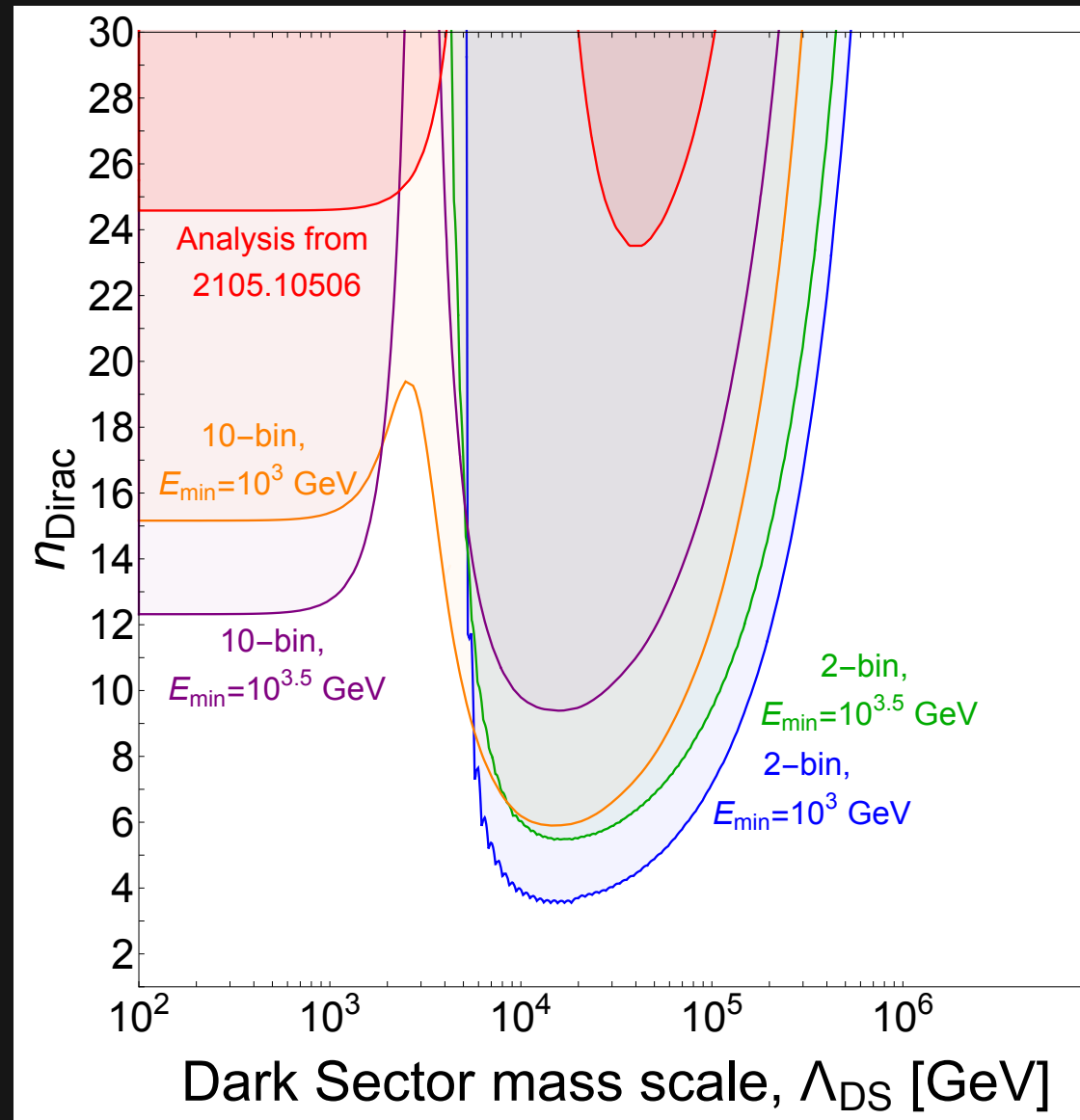
# Observational characteristics



# Observational characteristics



# Observational characteristics



# Summary

## Summary

Dark sector influences Hawking radiation

Existing & upcoming experiments searching for EBHs could  
probe dark sectors

Potentially sensitive to  $\mathcal{O}(10)$  Dirac fermions  
up to  $\sim 10^6$  GeV

# References

## References

Black hole evaporation: S.Hawking Nature 248, 30–31 (1974)

Primary radiation: T.Ukwatta et al.1510.04372

Secondary radiation using HDMSpectra: Capanema et al. 2110.05637

BlackHawk v2.0: A.Arbey, J. Auffinger 2108.02737

HDMSpectra: C.Bauer et al. 2007.15001

This project extends the analysis of M.Baker, A.Thamm 2105.10506v3

As far as I know, the idea of using Hawking Rad. to probe BSM DoF was introduced in 1510.04372, considering a single 5 TeV squark.



# Backup slides

## Backup Slides

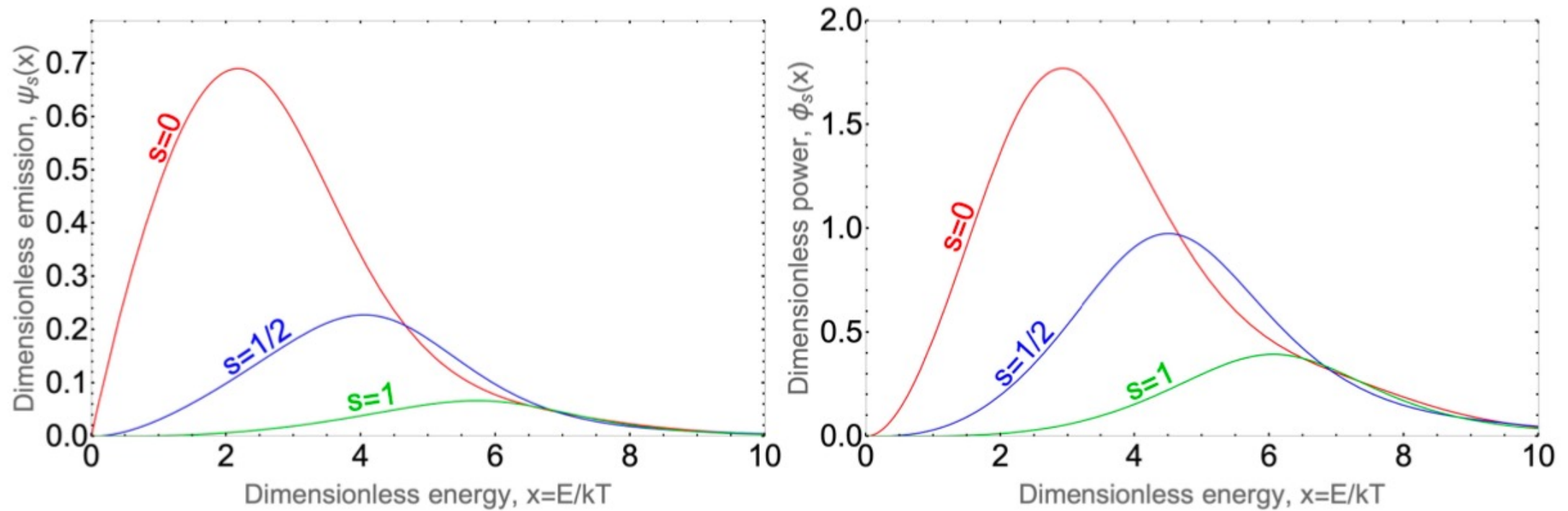


Figure 1.3:  $\psi_s(x)$  and  $\phi_s(x)$ , the dimensionless particle and power emission rates per DoF, respectively.

Made using BlackHawk

# Backup Slides

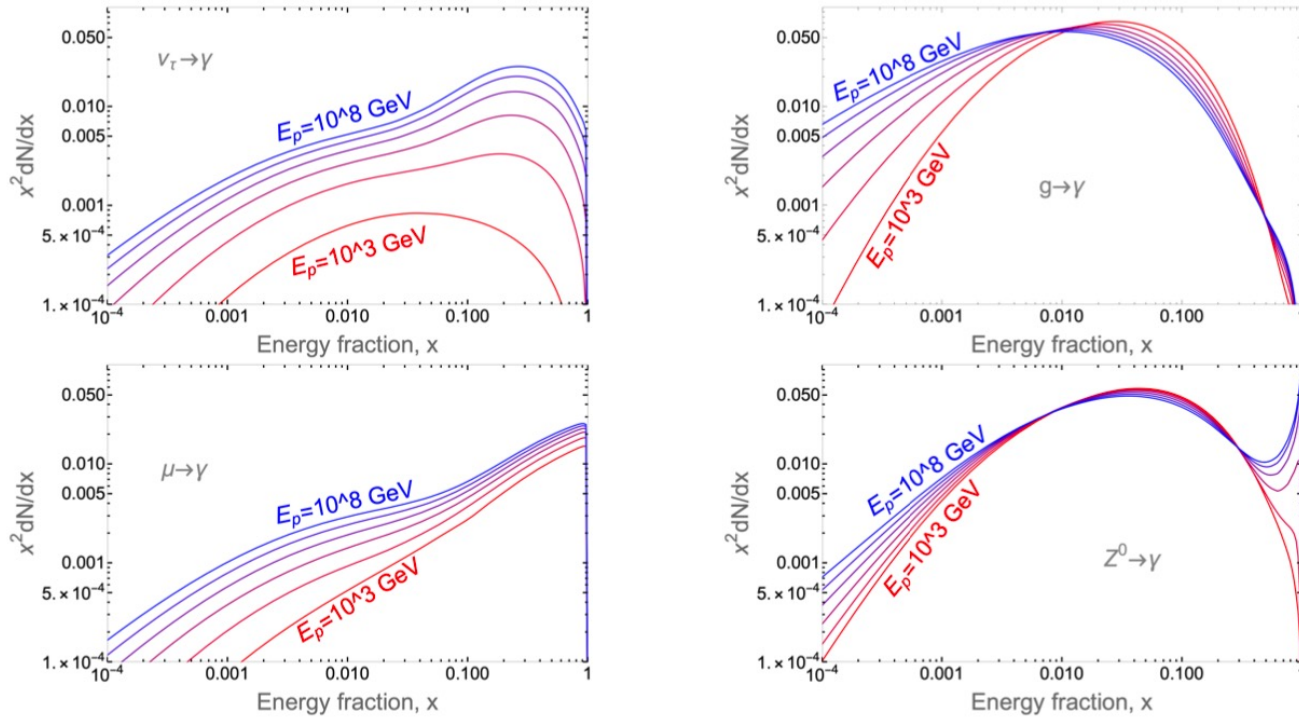


Figure 2.2: Examples of FFs for various primary species. The primary energies range from  $10^3$  to  $10^8$  GeV, red corresponding to lower  $E_p$  and blue to higher  $E_p$ . See Ref.[19] for more examples with different combinations of primary/secondary species. Note that the  $x$  values here refer to  $\bar{x}$  defined in the main text.

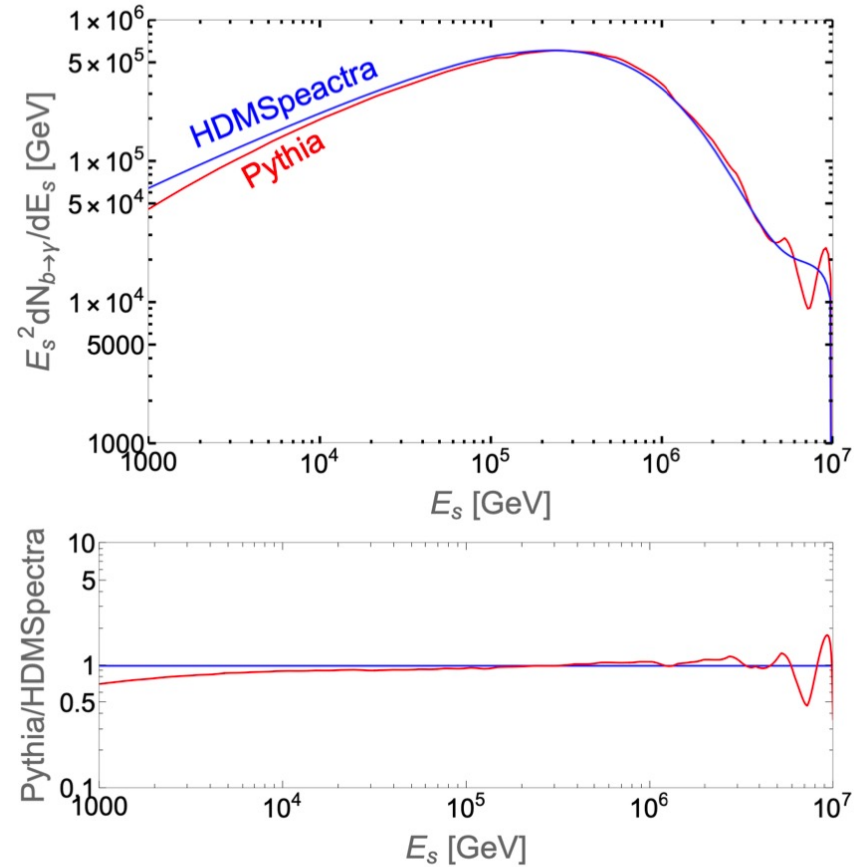


Figure 2.1: Comparison between fragmentation functions for  $b \rightarrow \gamma$  produced via Pythia and HDMSpectra, where  $E_p = 10^7$  GeV. The disagreement is almost always less than a factor of 2.

Made using HDMSpectra

## Backup Slides

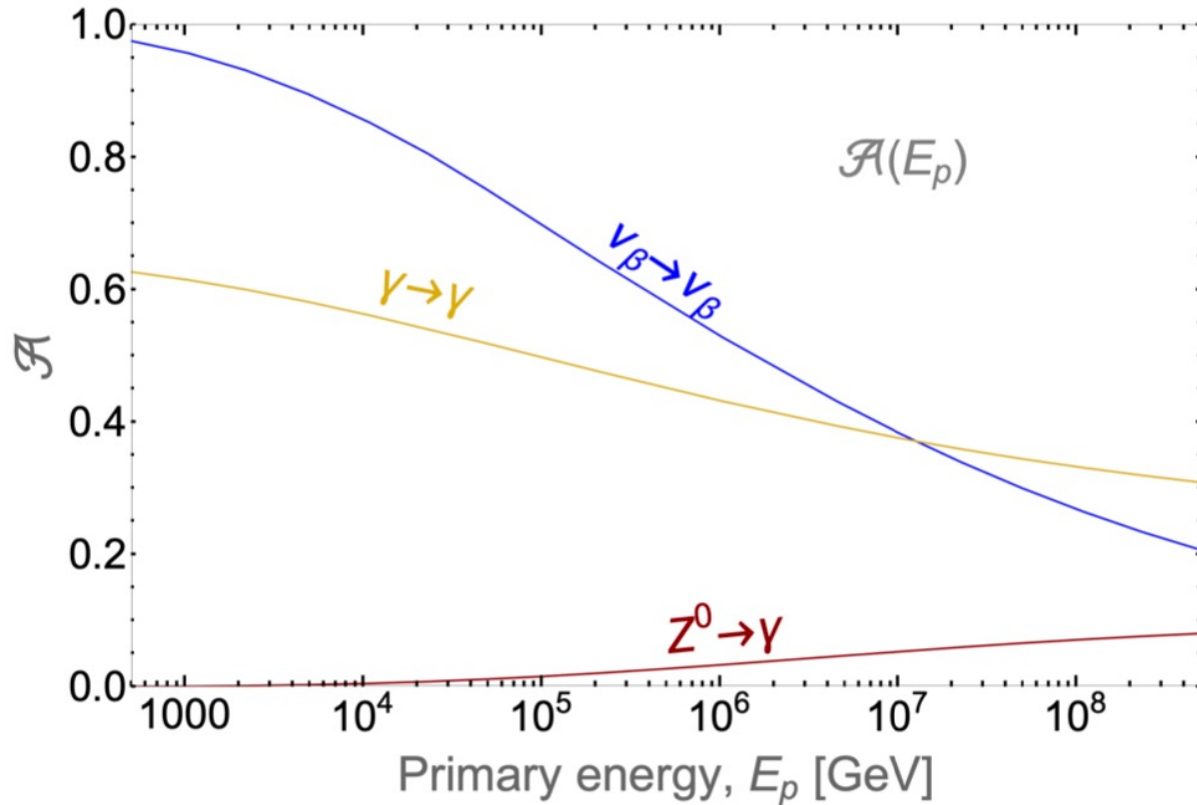


Figure 5.1:  $\mathcal{A}^{i \rightarrow f}(E_p)$  functions for primary  $i$  contributing to the total spectra of  $f$  with  $x = 1$ . Due to the relation between  $Z^0$  and  $\gamma$  as a result of electroweak symmetry breaking, the process  $Z^0 \rightarrow \gamma$  with  $x = 1$  at energies  $E_p \gg \Lambda_{EW}$  must be accounted for.

$$\frac{d^2 N_\gamma^{\text{total}}}{dE dt} = \frac{d^2 N_\gamma^{\text{sec}}}{dE_s dt} + \mathcal{A}^{\gamma \rightarrow \gamma}(E_p) \frac{d^2 N_\gamma^{\text{pri}}}{dE_p dt} + \mathcal{A}^{Z^0 \rightarrow \gamma}(E_p) \frac{d^2 N_{Z^0}^{\text{pri}}}{dE_p dt},$$

$$\left. \frac{d^2 N_{\nu_\beta}^{\text{total}}}{dE dt} \right|_{PBH} = \frac{d^2 N_{\nu_\beta}^{\text{sec}}}{dE_s dt} + \mathcal{A}^{\nu_\beta \rightarrow \nu_\beta}(E_p) \frac{d^2 N_{\nu_\beta}^{\text{pri}}}{dE_p dt},$$

$$\left. \frac{d^2 N_{\text{tot}}^{\nu_\alpha}}{dt dE} \right|_{\oplus} = \sum_{\beta=e}^{\tau} \sum_{i=1}^3 |U_{\alpha i}|^2 |U_{\beta i}|^2 \left. \frac{d^2 N_{\text{tot}}^{\nu_\beta}}{dt dE} \right|_{PBH}$$

Explanation for these can be found in Capanema et al. 2110.05637

Made using HDM Spectra

## Backup Slides

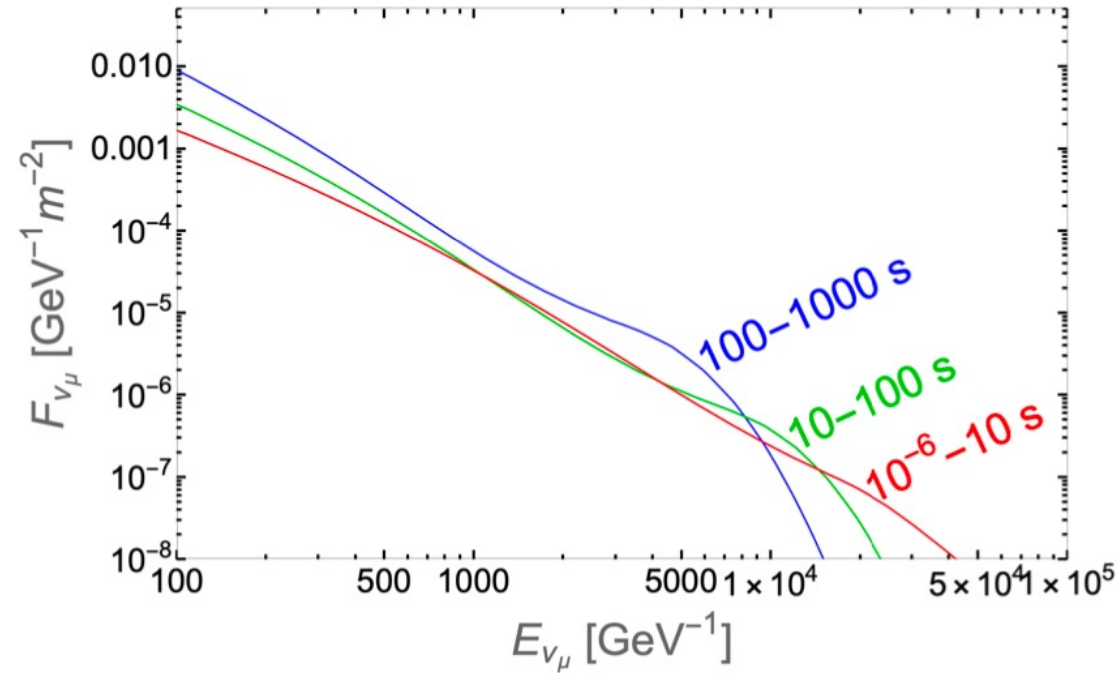
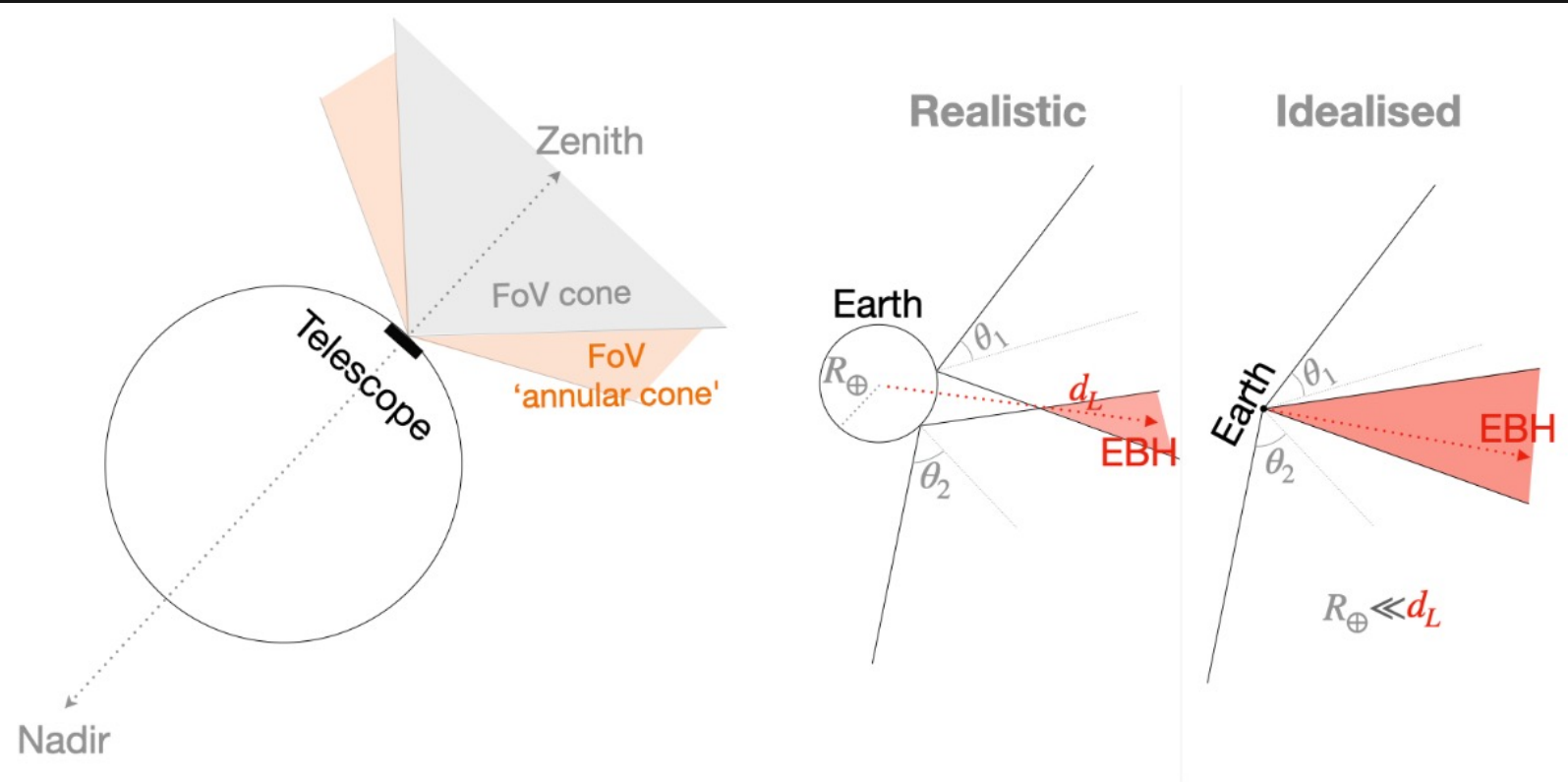


Figure 5.4: Fluences for  $\nu_\mu$  from an EBH 0.01 pc distant across the time intervals  $100 \text{ s} \leq \tau \leq 1000 \text{ s}$  (in blue),  $10 \text{ s} \leq \tau \leq 100 \text{ s}$  (in green), and  $10^{-6} \text{ s} \leq \tau \leq 10 \text{ s}$  (in red). We see that at lower energies the longer exposure time dominates over the greater emission rate at shorter times, but higher energies are only appreciably accessible at late times.

## Backup Slides



(a) The FoV of an experiment can be modelled by partitioning the full FoV into cones and annular cones with different effective areas. The Zenith and Nadir points are points on the celestial sphere 'above' and 'below' the experiment.

(b) Approximation used for the geometry of the FoV overlaps. Assuming the distance to the point of nearest intersection between overlapping FoVs is on the order of  $R_{\oplus}$ , then the FoV cones are assumed to share an apex.

Figure 4.5: Approximate geometric configuration used for the FoV overlaps.

## Backup Slides

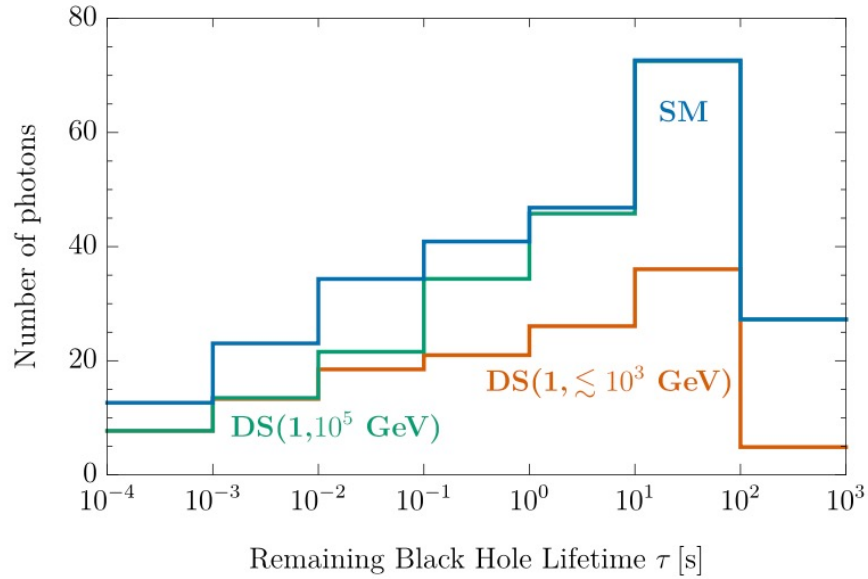


FIG. 3. The number of photons observed in each time window for an EBH observed at 0.01 pc for the SM and dark sector models at different mass scales.

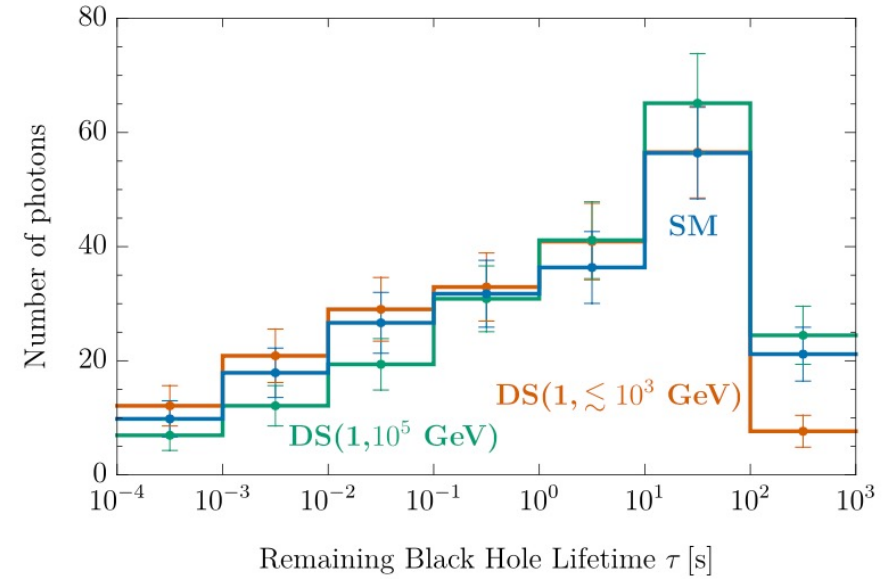


FIG. 4. The number of photons observed in each time window normalised to 200 total photons, for the SM and dark sector models at different mass scales. The error bars include statistical and 5% systematic errors.

Michael J. Baker and Andrea Thamm  
2105.10506v3

# Backup Slides

|  | HAWC   | LHAASO                | CTA South             | CTA North             | SWG0                      |
|--|--|-----------------------|-----------------------|-----------------------|---------------------------|
| Location [(°N,°E)]   | (19.0, -97.3)  | (29.4, 100.1)         | (-24.6, -70.4)        | (28.7, -17.9)         | (-24.2 – -13.5, ~-70)     |
| Field of View [sr]   | 0.64 ( $\theta_1$ band),<br>2.5 for all $\theta$ bands | 1.5–2                 | 0.019 – 0.069         | ***                   | 1.5–2 <sup>†</sup>        |
| Effective Area [m <sup>2</sup> ]   | $\sim 8 \times 10^4$                                   | $1.0 \times 10^6$     | $3.4 \times 10^6$     | $8.5 \times 10^5$     | $\sim 3.6 \times 10^5$    |
| Energy Resolution  | $\sim 23\%$ -40%                                       | $\sim 20\%$           | $\sim 5\%$            | ***                   | $\lesssim 30\%$           |
| Time Resolution  | $\mathcal{O}(100 \text{ ps})$                          | 0.5 ns                | ***                   | ***                   | ***                       |
| Angular Resolution   | 0.228°   | 0.25° – 0.33°         | $\lesssim 0.05^\circ$ | $\lesssim 0.05^\circ$ | $\sim 0.15^\circ$         |
| CR Rejection   | $2 \times 10^{-3}$                                     | $10^{-3}$ - $10^{-5}$ | $< 10^{-2}$           | $< 10^{-2}$           | $10^{-4}$                 |
| Background spectrum rate<br>at 20 TeV [Gev <sup>-1</sup> s <sup>-1</sup> ] | $2.8 \times 10^{-6}$                                   | $3.3 \times 10^{-5}$  | $1.8 \times 10^{-3}$  | $4.3 \times 10^{-3}$  |                           |
| Up-time  | $\sim 100\%$   | $\sim 100\%$          | ***                   | ***                   | $\sim 100\%$ <sup>†</sup> |
| Completion   | 2015   | 2021                  | 2025                  | 2025                  | R&D 2024                  |
| References   |  |                       |                       |                       |                           |

**Table 1.** <sup>†</sup> – our motivated assumption

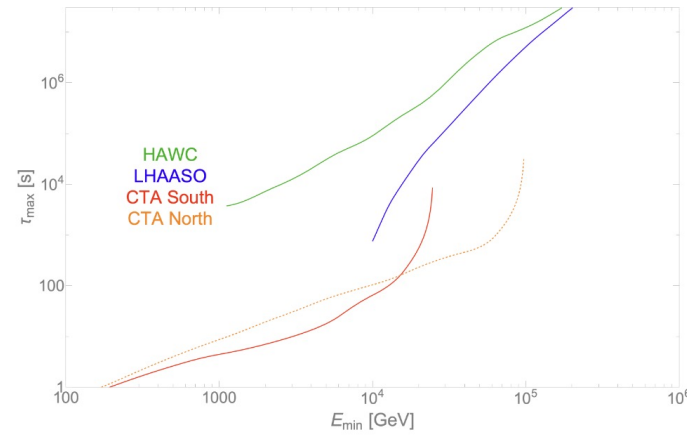
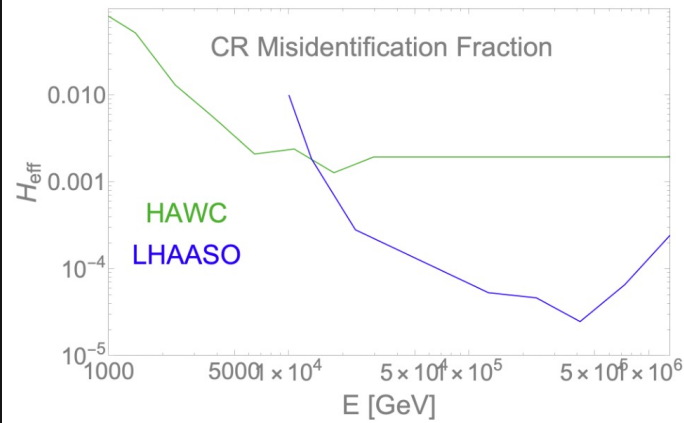
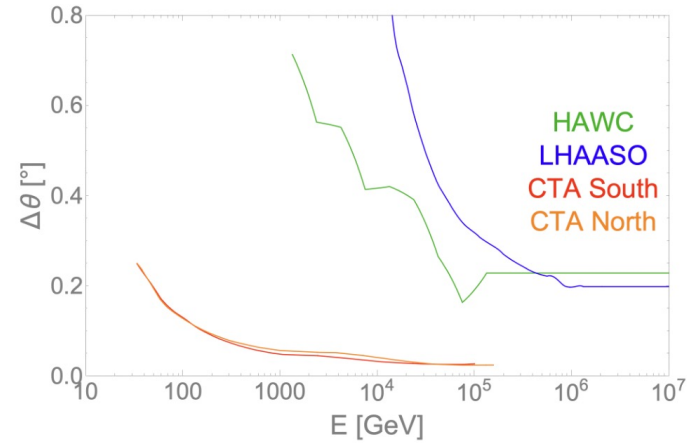
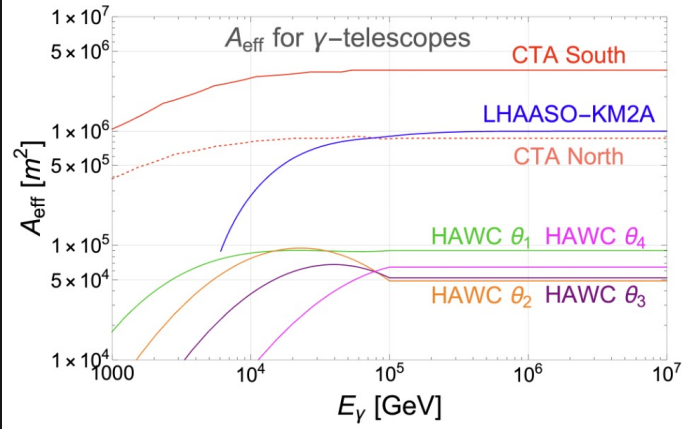


## Backup Slides

|                                  | IceCube Gen1 | IceCube Gen2 | KM3NET             |
|----------------------------------|--------------|--------------|--------------------|
| Location [(°N,°E)]               | (-90, 0)     | (-90, 0)     | (16, 36.3)         |
| Effective Area [m <sup>2</sup> ] | 89           | 700          | 130                |
| Time Resolution                  | ***          | ***          | ***                |
| Angular Resolution               | ~ 0.5°       | ***          | 0.1°               |
| Up-time                          | ~ 100%       | ~ 100%       | ~ 100%             |
| Completion                       | Operating    | 2033         | Under construction |
| References                       |              |              |                    |

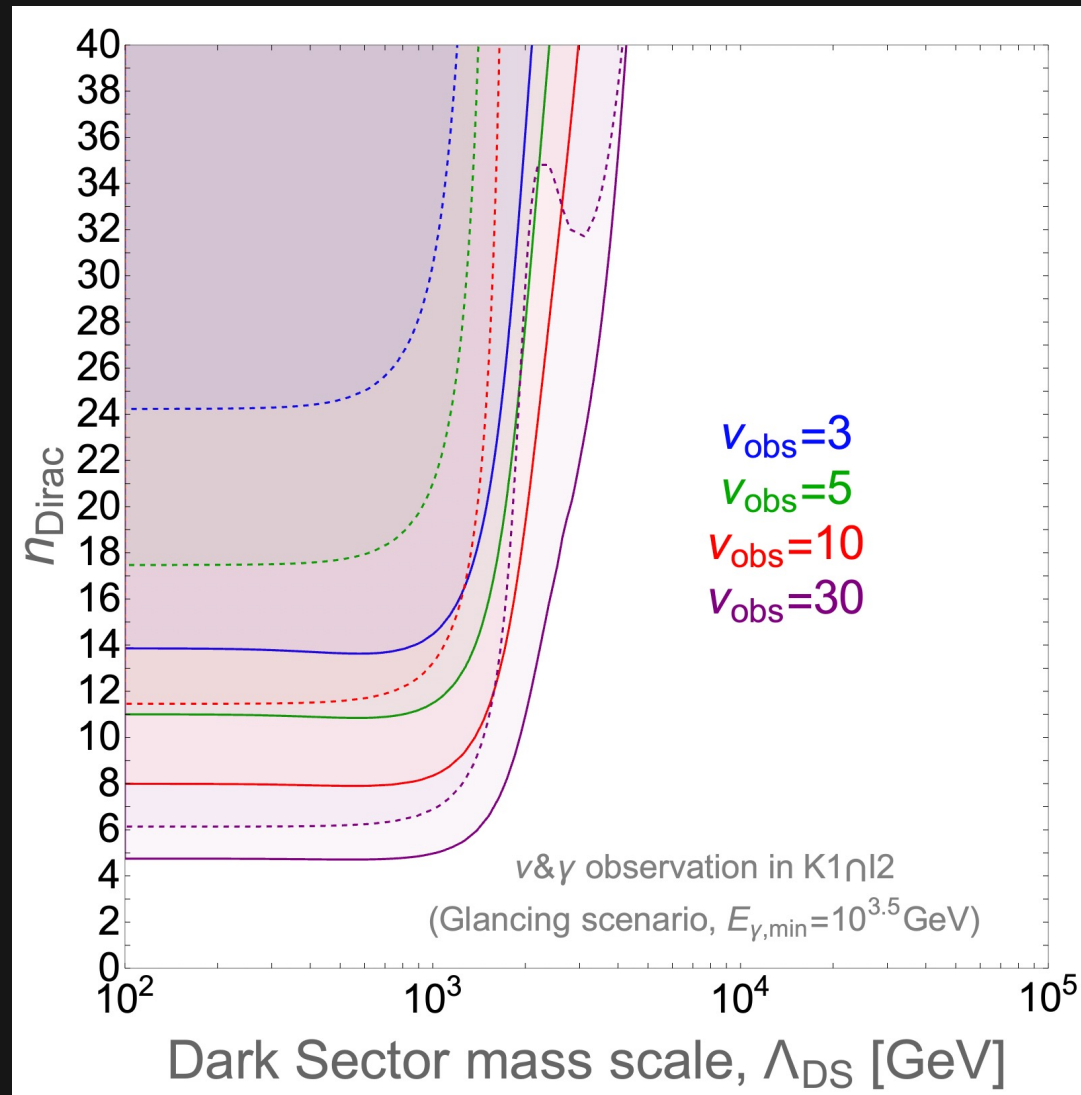
**Table 2.** NEUTRINOS

## Backup Slides

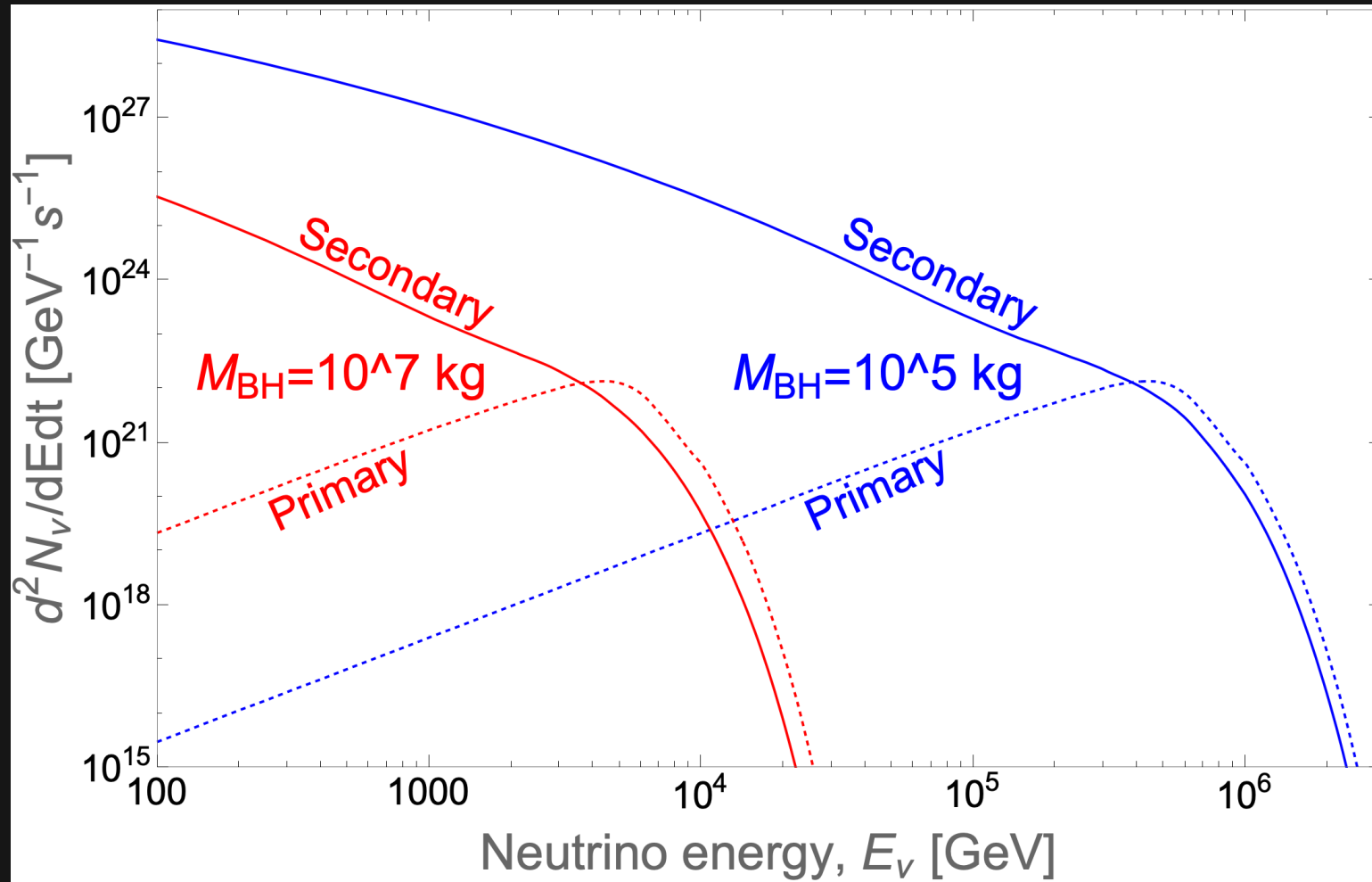


$$\tau_{\text{max}}^{-1} \simeq \int_{E_{\text{min}}}^{E_{\text{max}}} dE \frac{d\Phi}{dE}(E) A_{\text{eff}}^{(\text{H}+\text{He})}(E) 2\pi(1 - \cos(\Delta\theta(E))) \eta(E).$$

# Backup Slides



# Backup Slides



# Backup Slides

